The Human Prion Protein α2 Helix: A Thermodynamic Study of its Conformational Preferences

Barbara Tizzano,[1] Pasquale Palladino,[1] Antonia De Capua,[1] Daniela Marasco,[2] Filomena Rossi,[1,3] Ettore Benedetti,[1,3] Carlo Pedone,[2] Raffaele Ragone[4*] and Menotti Ruvo[2,4*]

[1]*Dipartimento di Chimica Biologica, Università "Federico II" di Napoli, Napoli, Italy*
[2]*Istituto di Biostrutture e Bioimmagini C.N.R., Napoli, Italy*
[3]*CIRPeB, Napoli, Italy*
[4]*Dipartimento di Biochimica e Biofisica, Seconda Università di Napoli, Napoli, Italy*

ABSTRACT **We have synthesized both free and terminally-blocked peptide corresponding to the second helical region of the globular domain of normal human prion protein, which has recently gained the attention of structural biologists because of a possible role in the nucleation process and fibrillization of prion protein. The profile of the circular dichroism spectrum of the free peptide was that typical of α-helix, but was converted to that of β-structure in about 16 h. Instead, below 2.1×10^{-5} M, the spectrum of the blocked peptide exhibited a single band centered at 200 nm, unequivocally associated to random conformations, which did not evolve even after 24 h. Conformational preferences of this last peptide have been investigated as a function of temperature, using trifluoroethanol or low-concentration sodium dodecyl sulfate as α- or β-structure inducers, respectively. Extrapolation of free energy data to zero concentration of structuring agent highlighted that the peptide prefers α-helical to β-type organization, in spite of results from prediction algorithms. However, the free energy difference between the two forms, as obtained by a thermodynamic cycle, is subtle (roughly 5–8 kJ mol^{-1} at any temperature from 280 K to 350 K), suggesting conformational ambivalence. This result supports the view that, in the prion protein, the structural behavior of the peptide is governed by the cellular microenvironment. Proteins 2005;59: 72–79.** © 2005 Wiley-Liss, Inc.

Key words: spongiform encephalopathy; α-helix; β-sheet; conformational ambivalence; circular dichroism; structuring agents

INTRODUCTION

A large number of human disorders, ranging from type II diabetes to Parkinson's and Alzheimer's disease, are associated with protein aggregation resulting from aberrant folding or processing events. In all these cases, aggregate formation may not only result in the absence of correctly functional protein, but also in cellular toxicity caused by the aggregate itself. Despite its fundamental biological importance, little is known about the molecular basis or specificity of the general phenomenon of protein aggregation, for which however a swapping mechanism based on hinge-bending motions has been recently hypothesized.[1] A common feature for all diseases is that proteins aggregate in a well-defined manner under appropriate conditions, but all efforts to elucidate these mechanisms at a molecular resolution have failed because of the highly aggregated state. Transmissible spongiform encephalopathies, also known as prion diseases, belong to this class. They are a group of unusual neurodegenerative disorders including new variant CJD (nvCJD), Gerstmann-Sträussler-Scheinker syndrome (GSS) and fatal familial insomnia (FFI) in humans, as well as scrapie in sheep and bovine spongiform encephalopathy (BSE) in cattle.[2,3] They are all characterized by a progressive neuronal degeneration. In almost all cases there is also a marked extracellular accumulation of an amyloidogenic conformer of the normal cellular prion protein (PrP^C), referred to as the scrapie isoform, PrP^{Sc},[2–4] which is thought to be responsible not only for the disease symptoms, but even for the infectivity.

PrP is a 231-amino acid ubiquitous glycoprotein whose physiological role is still elusive. Solution NMR studies of recombinant unglycosylated variants from four species[5–8] gave similar, prevailingly α-helical, monomeric folds, at different pH's,[9] which were presumed to represent the PrP^C general organization. The structures exhibit an N-terminal unfolded region and a C-terminal globular domain characterized by the presence of three α-helices (α1–α3), two short β-strands and a disulfide bridge between Cys^{179} and Cys^{214}, which connects α2 with α3 and confers structural stability. Studies by EM,[10] CD,[11] and FTIR techniques[12] suggest that PrP^{Sc} is characterized by a largely β-sheet content, suggesting that the conversion $PrP^C \rightarrow PrP^{Sc}$ should involve a major conformational transition affecting either the unfolded region or the α-helical domain. Recently, the 2.0-Å resolution crystal structure of the recombinant human prion protein has been reported.[13] The structure shows an unexpected three-dimensional (3D) domain swapping with a conforma-

*Correspondence to: Menotti Ruvo, Istituto di Biostrutture e Bioimmagini, CNR, Via Mezzocannone 6, 80134 Napoli, Italy. E-mail: ruvo@chemistry.unina.it and Raffaele Ragone, Dipartimento di Biochimica e Biofisica, Seconda Università di Napoli, via S. Maria di Costantinopoli 16, 80138 Napoli, Italy. E-mail: ragone@unina2.it

Received 28 September 2004; Accepted 25 October 2004

Published online 1 February 2005 in Wiley InterScience (www.interscience.wiley.com). DOI: 10.1002/prot.20395

tional switch region located at the dimer interface centered on residues 190–195, which, as suggested by the authors, could represent a sort of snapshot of the first stage of the structural transition. Despite the strong differences in tertiary structure (dimers are held together by two disulfide bridges obtained by rearrangement of the only one described in the monomers), local folds in the X-ray and NMR structures are globally retained, with considerable differences observed only in proximity of the C-terminal side of α2 which is partly converted to a short beta strand. The true mechanism of PrP^{Sc} formation under physiological conditions is at present still unknown, but biochemical evidence demonstrates that conversion does not occur through a disulfide scrambling-driven covalent oligomerization,[14] so this X-ray structure has been largely questioned and the covalent dimerization explained as an artifact produced by the crystallization conditions (pH 8.0, 3 M NaCl).[13] Nevertheless, the appearance of a β-sheet in a limited region, where some familial prion disease mutations map[15] and where an unusual Thr-rich sequence is present, is quite intriguing. What makes this observation even more interesting is that the newly formed β-sheet contributes to dimer stability, maybe favoring its formation. These observations, along with the presence of threonines, a β-branched amino acid with a strong β-sheet-forming propensity,[16] could suggest that some conformational weaknesses, which can affect the whole protein architecture, converge on the short sequence 190–195 or a more limited surrounding region, and that can help promote the noncovalent association of two misfolded monomers.

Synthetic variants of the α2 helix have been already studied to assess fibrillization capabilities,[17] cellular toxicity,[11] and metal binding properties,[18] and all data point to an important role of the region in the overall biological behavior of the whole prion protein, mainly in presence of Cu(II) ions.[18] A hypothetical structural change involving this region, induced or facilitated by unknown external factors (metals, protein-X), could therefore promote a β-sheet-mediated protein association leading to a further α → β transition and consequently to aggregation.

During the writing of this paper, the crystal structure of the sheep prion protein was described.[19] Interestingly, the protein, which shares more than 90% identity with the human variant, has a monomeric structure very close to that determined in solution by NMR on the same and other variants. From the protein crystal structure, not yet available in the protein data bank, and harnessing information derived from lattice protein–protein interactions, the authors identify the threonine-rich region 188–200, encompassing the C-terminal side of α2 and the N-terminal side of α3, as a site of local instability and possibly of β-sheet nucleation. They also propose that protein oligomerization takes place through association of β-sheets, which then synergically propagate involving other regions of the molecule. These observations confirm and strengthen our hypothesis about a role of α2 in prion molecular rearrangement. To further support this hypothesis, we have studied the conformational behavior in solution of the whole α2 helix, encompassing residues from Asn173 to Gly195, in its C-terminal amide and N-terminal acetylated form (blocked). In order to define its intrinsic structural propensities and to selectively determine the thermodynamics that regulate a possible conformational conversion, the peptide model has been accurately chosen on the basis of the available protein structures, minding that other residues from the interconnecting loops or distant in the sequence, which might contribute to helix stability only in the whole protein, were not included.

MATERIALS AND METHODS

Peptide Synthesis and Characterization

All solvents were reagent grade. HPLC chemicals were purchased from Lab-Scan (Dublin, Ireland), while other organic reagents were from Sigma-Aldrich (Milan, Italy). N-α-Fmoc protected amino acids and the activating agents were purchased from Inbios (Pozzuoli, Italy). Resins for peptide synthesis were from Novabiochem (Läufelfingen, CH). Columns for peptides purification and characterization were from Phenomenex (Torrance, CA).

Peptides (NNFVHDCVNITIKQHTVTTTTKG and N- and C-blocked, Ac-NNFVHDCVNITIKQHTVTTTTKG-NH_2) were synthesized in batch by standard Fmoc chemistry protocol on WANG or Rink-amide MBHA resins. Acylations were carried out in 50% DCM/DMF for 15 min using PyBOP/DIEA (1:2) as activating agents (without preactivation) with a four-fold amino acid excess. Fmoc removal was achieved by 30% piperidine/DMF treatment for 10 min. After peptide assembling, acetylation was carried out where requested, by treatment with a 1 M solution of acetic anhydride in DMF containing 5% DIEA. Cleavage from the solid support was achieved by treatment with a trifluoroacetic acid (TFA)/triisopropylsilane (TIS)/water (90:5.0:5.0 v/v/v) mixture for 90 min at room temperature. Then, peptides were precipitated in ether, dissolved in water/acetonitrile (1:1 v/v) mixture, lyophilized, and purified by RP-HPLC using a Jupiter C_{18} Jupiter 250 × 22 mm ID column (15 μm, 300 Å) applying a linear gradient of acetonitrile in 0.1% TFA from 10% to 60% in 50 min. Peptide purity and integrity were confirmed by RP-HPLC analysis using analytical columns (Jupiter C_{18}, 250 × 4.6 mm ID,15 μm, 300 Å) and by MALDI-TOF mass measurements (Voyager-DE Biospectrometry Workstation, PerSeptive Biosystems).

Secondary Structure Prediction

Secondary structure prediction of the peptide corresponding to the second helical region of the globular domain of human prion protein was performed according to Jones[20] using the PSIPRED server facility available at http://bioinf.cs.ucl.ac.uk/psipred.[21] Moreover, the helical behavior of the peptide was analyzed by the Agadir algorithm based on the helix to coil transition theory.[22–25]

Circular Dichroism (CD)

Sodium dodecyl sulfate (SDS) and 2,2,2-trifluoroethanol (TFE) were obtained from Sigma-Aldrich (Milano, Italia) and Romil LTD (Dublin, Ireland), respectively. The working concentration of SDS was chosen on the basis of its

critical micelle concentration (cmc) at room temperature.[26–28] Far UV CD spectra were recorded for both free and blocked peptide dissolved in 10 mM phosphate buffer, pH 7.2. Optimal working concentrations were determined in preliminary experiments by acquiring CD spectra at different concentrations (room temperature) while keeping constant the number of peptide molecules in the optical path. This was achieved by diluting a 10^{-4} M peptide stock solution and simultaneously increasing the cell pathlength by a factor equal to the dilution factor. CD spectra were recorded at regular time intervals in order to monitor possible spontaneous changes due to aggregation and/or fibril formation. For all concentrations explored, the free peptide showed the typical two-minima α-helix spectrum, which, after 16 h, completely converted to the classical β-structure appearance with a maximum at around 195 nm and a minimum at around 215 nm, suggesting a marked peptide association or aggregation. The blocked peptide was found to aggregate time-dependently above a concentration of about 2.1×10^{-5} M. Below this concentration, the spectra exhibited a single band centered on 200 nm, unequivocally associated to random conformations, which did not evolve even after 24 h, showing only a limited intensity reduction. Given its stability in solution, the blocked 173–195 prion peptide, henceforth called PrP[173–195] was used throughout the experiments at a concentration of 10 μM, as measured by absorbance at 257.5 nm, assuming a molar extinction coefficient of 195 $M^{-1} \times cm^{-1}$ for phenylalanine.[29]

On this peptide, TFE and SDS titration experiments were carried out using quartz cells with 10-mm pathlength and scanning spectra from 190 to 260 nm on a Jasco J-715 spectropolarimeter equipped with a thermostated water bath. Instead of carrying out isothermal titrations by adding increasing volumes of structuring agent to the peptide solution, which usually results in large errors due to dilution, we prepared a number of peptide solutions in 10 mM phosphate buffer, pH 7.2, containing a fixed concentration of structure-inducing substance. Then, for each concentration of structuring agent, far UV CD spectra were isothermally recorded at increasing temperature steps over the interval 283–343 K. Each spectrum was obtained averaging three scans, subtracting contributions from structuring agents, and converting the signal to mean residue ellipticity in units of $deg \times cm^2 \times dmol^{-1} \times res^{-1}$. Other experimental settings were: 20 nm/min scan speed, 2.0 nm band width, 0.2 nm resolution, 50 mdeg sensitivity, and 4 sec response. To monitor the possible formation of disulfide-bridged dimeric peptides, which could then affect CD determinations, HPLC analyses were carried out on peptide solutions from all experiments. Only very small amounts of dimer were observed in the different samples, up to a maximum of around 10% in the worst case, so no DTT or other reducing additives were used.

Treatment of Data

For either set of experiments, we assumed a two-state model and evaluated free energy changes for the disorder-to-order transition, extrapolating isothermal titration data to zero concentration of structure-inducing substance. To warrant homogeneity of calculations at different temperatures, the concentration of TFE or SDS was always expressed in molal units. In any case, we implemented pertinent equations in the general-purpose non-linear fitting program Scientist from MicroMath Software (San Diego, CA), as described below.

For TFE, the ellipticity at 222 nm (Θ_{222}) was analyzed using a six-parameter model analogous to that previously derived for absorption[30] or fluorescence denaturation,[31] which assumes a linear dependence of pre- and post-transition baselines on the TFE concentration, according to the function:

$$\Theta_{222} = \{\Theta_r^\circ + m_r C + (\Theta_\alpha^\circ + m_\alpha C)\exp[-(\Delta G_\alpha^\circ + mC)/(RT)]\}/\{1 + \exp[-(\Delta G_\alpha^\circ + mC)/(RT)]\} \quad (1)$$

Here, the TFE concentration is given by C, the pretransition dichroic signal intercept (0% TFE) and slope are Θ_r° and m_r, respectively, the helical state dichroic signal intercept and slope are Θ_α° and m_α, respectively, the secondary structure formation free energy function intercept and slope are ΔG_α° and m, respectively, R is the universal gas constant, and T represents the absolute temperature.

For SDS, the ellipticity at 200 nm (Θ_{200}) was analyzed using a function analogous to that adopted for TFE, but the slopes of pre- and post-transition baselines were set to zero and the dependence of the free energy on the detergent concentration was analyzed by a binding isotherm, according to the five-parameter equation:

$$\Theta_{200} = \{\Theta_r^\circ + \Theta_\beta^\circ \exp[-\Delta G_\beta^\circ/(RT) + \Delta n \ln(1 + kD)]\}/\{1 + \exp[-\Delta G_\beta^\circ/(RT) + \Delta n \ln(1 + kD)]\} \quad (2)$$

Here, the SDS concentration is given by D, and the 0% SDS and β-state dichroic signal intercepts are Θ_r° and Θ_β°, respectively. The free energy of secondary structure formation in absence of SDS is given by ΔG_β°, and Δn represents the excess of the peptide detergent binding sites in the β-state characterized by the intrinsic binding constant k. Owing to the strong correlation between k and Δn, curve fitting was carried out using $k = 50000\ M^{-1}$, which is the value found for SDS interaction with electrostatic binding sites of small proteins.[32] This model has already been shown to work for micellar aggregation[33] and is under further development in our laboratory (Ragone et al., unpubl. obs.).

RESULTS

Secondary Structure Predictions

The peptide fragment corresponding to the second helical region of the globular domain of human prion protein was analyzed by CD spectroscopy in order to determine its tendency to adopt different secondary structures and assess its capability to undergo an α → β transition under suitable conditions. The peptide structural preferences were first examined by prediction algorithms, as described in Materials and Methods. Figure 1 highlights that, according to the chosen method, all residues are predicted to be in

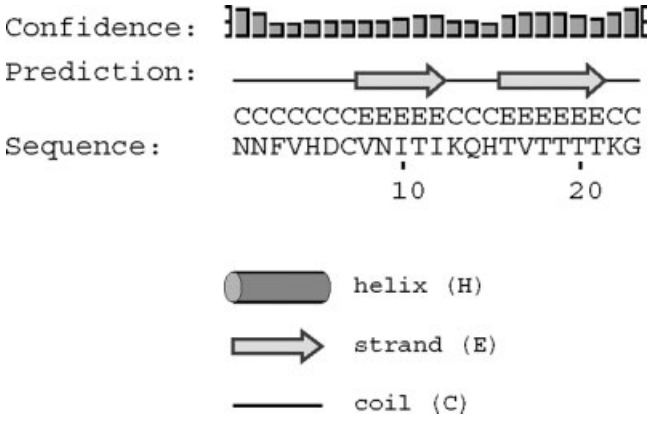

Fig. 1. Secondary structure prediction of PrP [173–195]. The prediction was obtained by the PSIPRED server, available at http://bioinf.cs.jucl.ac.uk/psipred.

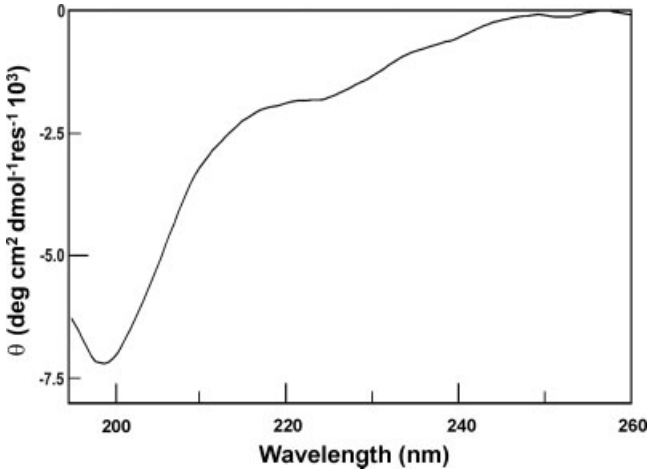

Fig. 2. Far UV CD spectrum of PrP [173–195]. The spectrum, obtained at a concentration of 10 μM, is characterized by a strong negative band near 200 nm and a negative shoulder at around 220 nm, which suggests random organization.

nonhelical conformation. Furthermore, calculation of the percentage helicity of the blocked peptide sequence by the semi-empirical helix-propensity-specific algorithm Agadir predicted that less than 22% residues are organized in α-helix at any temperature in the liquid water range. Although these predictions are in contrast with the α-helical organization found in the normal cellular prion protein, they are in substantial agreement with the far UV CD spectrum of PrP[173–195], which, at neutral pH and at concentrations where no aggregation is detected, shows the profile typical of disordered structure, i.e., a strong negative band near 200 nm and a negative shoulder at around 220 nm[34] (Fig. 2). Because of a possible involvement in the nucleation process of β-structure formation, we were prompted to thoroughly analyze the conformational preferences of this peptide fragment, monitoring structural modifications caused by α- or β-inducing agents and measuring the associated free energy differences.

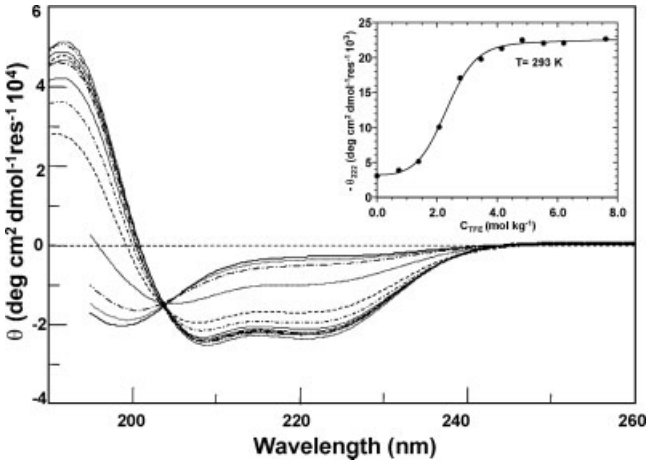

Fig. 3. TFE titration. Far UV CD spectra of PrP [173–195] are superimposed as a function of TFE concentration (from top to bottom, 0–7.7 mol kg^{-1}, according to data points in the inset). The inset shows the effect of TFE as monitored by the dichroic activity at 222 nm; T = 293 K.

TFE Titrations

The first set of experiments was carried out monitoring TFE-induced modifications of the far UV CD spectrum of PrP[173–195] at different temperatures, as described under Materials and Methods. TFE is a hydrophilic and hydrogen-bonding solvent that appears to stabilize peptides in the secondary structure for which a given sequence has propensity.[35] It belongs to a group of organic substances such as methanol, ethanol, acetonitrile, 1,1,1,3,3,3-hexafluoroisopropanol at low pH, octanol mixed with other alcoholic solvents, and SDS at high concentrations, which are known to induce α-helical organization in peptides.[36–38] In presence of about 40% TFE, the spectra at different temperatures assumed the typical appearance of helical structures, with pronounced minima at 208 and 222 nm and a strong positive maximum at 191–193 nm,[34] and showed a well defined isodichroic point at 205 nm (Fig. 3), indicative of two-state behavior. Therefore, after verifying the reversibility of this structural modification by dilution, dichroic activity data as a function of the TFE concentration (Fig. 3, inset) at different temperatures were recorded and treated according to Equation 1. This equation assumes that the free energy of helix formation linearly depends on the concentration of TFE in the solution, i.e., $\Delta G^{\circ}_{\mathrm{TFE}} = \Delta G^{\circ}_{\alpha} + mC$, and is therefore analogous to the relationship adopted to extrapolate the unfolding free energy to zero denaturant concentration, which has been shown to be valid for the structuring action of TFE as well.[39–41] This allowed us to obtain the extrapolated transition free energy ($\Delta G^{\circ}_{\alpha}$) at zero concentration of structuring agent, which was estimated to be 11–14 kJ-mol^{-1} in the range 280–350 K.

SDS Titrations

A similar set of experiments was carried out using SDS as the structuring agent, based on the notion that peptides may be induced into a β-sheet structure at sub-micellar concentrations of this substance.[35,42,43] Actually, little is

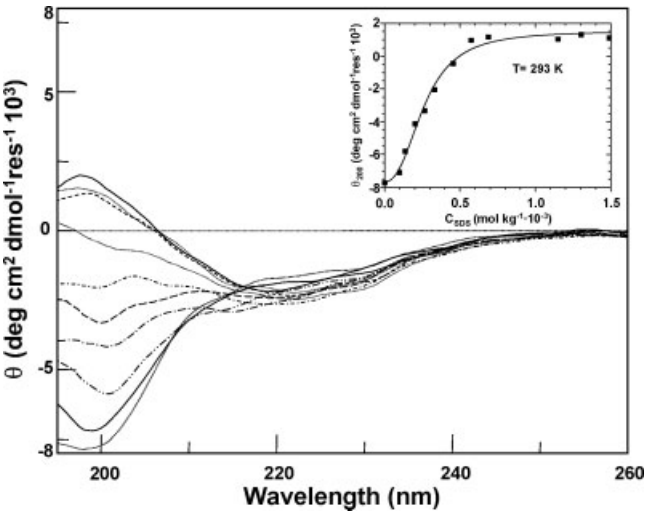

Fig. 4. SDS titration. Far UV CD spectra of PrP [173–195] are superimposed as a function of SDS concentration (from bottom to top, 0–1.15 mmol kg^{-1}, according to data points in the inset). The inset shows the effect of SDS as monitored by the dichroic activity at 200 nm; T = 293 K.

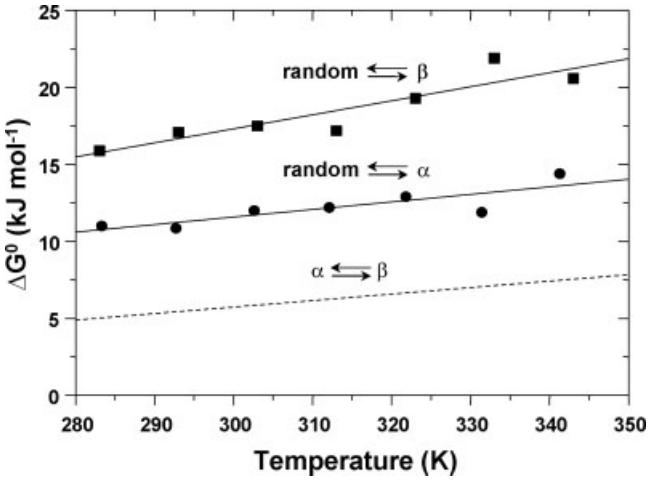

Fig. 5. Thermodynamic analysis of structural preferences of PrP [173–195]. Extrapolated values of $\Delta G°$ for the random-to-α and random-to-β transitions are plotted as a function of temperature. The dashed line represents the thermodynamics of the α → β transition as obtained by difference between the $\Delta G°$'s of the two random-to-ordered structure transitions. All experimental data were fitted to straight lines because neither transition is accompanied by an appreciable heat capacity change, suggesting that enthalpy and entropy changes are independent of temperature.

known about the nature of this solvent system, which has been described as a mimetic of protein interiors. It is presumed that the nonpolar tails provide a template for the hydrophobic domains of peptides, mimicking the environment found in the interior of the parent protein, whereas the sulfate moiety keeps the β-structured peptide in solution. The addition of SDS reversibly led to spectra with positive and negative bands near 195–200 nm and 216–220 nm, respectively, which can be ascribed to a β-type profile.[34] Moreover, a blurred isodichroic point can be perceived between 211 and 216 nm (Fig. 4), suggestive, as in the case of TFE, of a two-state equilibrium. Unfortunately, we could not obtain better definition of these spectral features, because the signal weakens above the cross point between the spectra of the two species, merging with the instrumental noise. Then, for each temperature assayed, the dichroic activity at 200 nm was fitted to Equation 2 to obtain the transition free energy ($\Delta G°_{\beta}$) in the absence of SDS (Fig. 4, inset).

The binding isotherm that describes the dependence of the free energy on the detergent concentration, i.e. $\Delta G°_{SDS} = \Delta G°_{\beta} + RT\ln(1 + kD)^{\Delta n}$, assumes that the peptide molecule possesses a discrete number of identical and noninteracting binding sites for SDS. It is therefore analogous to the model used for denaturation curves of proteins, better known as the denaturant binding model.[44,45] This formulation leads to thermodynamic inconsistencies when it is applied to very weak binding, such as is found with protein denaturants, but it is accurate in the present case, where few distinct independent binding sites of high strength (positively charged residues are well separated in the sequence) are reasonably generated during the conversion from the unbound- to the SDS-bound-peptide molecule.[46] Formally, the binding of ionic surfactant to water-soluble proteins occurs through two sets of binding sites, electrostatic (higher affinity) and nonpolar (lower affinity). It is therefore conceivable that the driving force for peptide secondary structure organization at the low SDS concentrations employed in our experiments could be the presence of more exposed cationic binding sites in the β-state that, on the average, are less available in the disorganized form. In fact, calculations gave $2.5 < \Delta n \leq 3$ at any temperature, which is in good agreement with the number of positively charged side chains in the peptide (two lysines and two histidines). The estimated $\Delta G°_{\beta}$ for the conversion $PrP[173–195]_{unfolded} \rightarrow PrP[173–195]_{\beta\text{-structure}}$ is 16–22 kJ mol^{-1} in the range 280–350 K, which is higher than that found for the $PrP[173–195]_{unfolded} \rightarrow PrP[173–195]_{\alpha\text{-helix}}$ transition.

Thermodynamic Analysis

Figure 5 provides a comprehensive thermodynamic view on the structural preferences of PrP[173–195], as they emerge from the above described experiments. First of all, we have assessed the reliability of these free energy estimates calculating the α- or β- propensity ($\langle CP \rangle = e^{-\Delta G°/(NRT)}$, with $N = 23$) of an average amino acid residue in PrP[173–195]. To allow a comparison with other scales, these conformational preferences have been expressed as an energy-like term, $E = -\log\langle CP \rangle$, keeping in mind that E will take negative values for a residue that favors a given conformation, and positive otherwise. At 20°C, our average propensities of 0.08 and 0.13 for α-helix and β-sheet, respectively, are in good agreement with the RAN scale previously published,[47] confirming the reliability of our procedure and, more importantly, a small preference of the peptide to assume α-conformations. Figure 5 also shows how we have derived the thermodynamic parameters characterizing the α → β transition using free energies estimated by TFE- and SDS-induced transitions. It is worth noting that neither set of free energy data shows

any significant curvature, i.e. neither transition is accompanied by an appreciable heat capacity change, suggesting that enthalpy and entropy changes are independent of temperature. Accordingly, for each transition, we have performed a linear regression of free energy versus temperature data to estimate the thermodynamics of the α → β transition by difference. As a result, the α-form is more stable than the β-form by roughly 5–8 kJ mol^{-1} at any temperature from 280 K to 350 K, as can be calculated by regression intercept and slope, which equal −6.9 kJ mol^{-1} and −0.04 kJ mol^{-1} K^{-1} and represent temperature-independent enthalpy and entropy differences, respectively.

DISCUSSION

The comprehension of the structural organization of PrP^{Sc} is one of the most intriguing and stimulating topics of the last decade. Although reasonable models have been proposed for it,[10] a definitive PrP^{Sc} structure is presently not available since its elucidation is hindered by the highly aggregated state. A number of studies have also aimed at enlightening the molecular mechanism by which the PrP^{C} → PrP^{Sc} conversion is triggered, since it could help to derive a model and, of course, to propose a means to conversion blockade. Among the others, the involvement of pH changes or high metal ions concentrations has been proposed,[18] as well as the presence of sites of intrinsic local protein instability.[13,19] This last aspect has been largely investigated also in view of the known pathogenic PrP mutations which are responsible of the inherited variants of the disease.[15,48,49]

Many investigations have been reported on protein fragments reproducing different portions of the full-length molecule, but detailed structural studies have been often hampered by the aggregation tendency of peptides.[50] In this work we have been concerned with both free and terminally-blocked peptide corresponding to the second helical region of the globular domain of human prion protein, PrP[173–195], which has recently gained the attention of structural biologists[13,17,19] because of a possible role in the nucleation process of PrP oligomerization and therefore fibrillization. The strong tendency of the peptide to aggregate did not allow us to perform any conformational analysis by NMR techniques, in fact peptide solutions at even 0.2 mM exhibited a marked band broadening and signal reduction in less than 3 h (data not shown). The peptide, at near neutral pH and in both the free and blocked version, showed time-dependent aggregation properties even at lower concentrations (up to 21 μM) which, as reported earlier,[17] are likely exacerbated by the presence of the free thiol group. This behavior, for the blocked variant only, was absent below this threshold, allowing us to determine thermodynamic parameters associated to peptide rearrangement in solution. Although the isolated peptide is randomly structured in buffer solution, we have been able to get reasonable estimates of its conformational preferences by analysis of TFE- or SDS-induced modifications, deriving the $\Delta G°$ and the average propensity of α- and β-structure formation as a function of temperature. By difference between the two sets of measurements, we have estimated that a small free energy separates the two conformations, which denotes structural ambivalence of the peptide in the conditions explored. It has been suggested that the inherent property of a peptide to fold into either the α- or β-conformation is likely under the control of environmental changes.[51,52]

In this regard, contrarily to the secondary structure prediction, the analysis of experimentally-derived structural propensities provides evidence that a small, but significant entropic advantage of 0.04 kJ mol^{-1} K^{-1} allows the PrP[173–195] peptide to adopt an α-helical organization over a temperature interval that includes the physiological condition, even when it is not embedded in the normal cellular prion protein. At the same time, we guess that the subtle free energy difference between the α and β form might allow this structural ambivalence of the peptide to be governed, in the protein, by the cellular microenvironment. It should be noticed that, in the whole protein, the α2 first three turns are closely packed against the α3, generating an extensive complementary interface[13,19] which strongly stabilizes the helix up to around residue 188, with a further contribution to stabilization provided by the presence of the glycosyl moiety on the Asn181.[17] Conversely, the region spanning residues 190–195 is rather apart from the last helix, is poorly defined in the NMR structures,[49] and is found in β-conformation in the dimeric crystal structure of human prion protein, suggesting that this site of the protein is one of the most prone to structural rearrangements or modifications upon suitable perturbations. In light of these observations, our results could suggest that the conformational fragility associated to the full length helix 2 could actually be focused on its short C-terminal end, which, in cooperation with other sites in the N-terminal region (fragment ~90–140),[53] could be involved in the nucleation process of prion misfolding and oligomerization.[19] This hypothesis is strengthened by the observation that fragment 180–195 assumes a β-conformation in aqueous buffer at neutral pH (as determined by CD), which is invariably retained under a large variety of conditions, including 50% TFE. By converse, the complementary fragment 173–179, under the same conditions, shows typical α-helical spectra (Ronga et al., manuscript in preparation). We also hypothesize that structural perturbations leading to molecular rearrangements could involve the binding of His187 by copper ions[18] and/or the deglycosylation of Asn181,[54] which has been shown to strongly destabilize this helical region[17] and to lead to enhanced fibril formation and toxicity.

Our conclusions are in substantial agreement with previous reports about the possible role of the PrP[173–195] segment in the conversion of PrP^{C} into fibrillar PrP^{Sc}. As a novelty, the present work provides a thermodynamic basis to previous structural investigations on the relative stability of this region of the protein, even though it is based on the peptide fragment assumption. Moreover, our approach permits to highlight possible structural ambivalence as a function of temperature, a feature that, to the

best of our knowledge, has never been experimentally assessed before in a 23-residue-long peptide.

ACKNOWLEDGMENTS

The authors acknowledge Ministero dell'Istruzione, dell'Università e della Ricerca (M.I.U.R.) COFIN 2003 (Prot2003 031424) and FIRB 2003 N° RBNE01ARR4_002, and the National Research Council (C.N.R.) of Italy for their support to this research.

REFERENCES

1. Sinha N, Tsai C-J, Nussinov R. A proposed structural model for amyloid fibril elongation: domain swapping forms an interdigitating β-structure polymer. Protein Eng 2001;14:93–103.
2. Prusiner SB. Prions. Proc Natl Acad Sci USA 1998;95:13363–13383.
3. Horwich AL, Weissman JS. Deadly conformations-protein misfolding in prion disease. Cell 1977;89:499–510.
4. Pan KH, Baldwin M, Nguyen J, Gasset M, Serban A, Groth D, Mehlhorn I, Huang Z, Fletterick RJ, Cohen PE, Prusiner SB. Conversion of alpha-helices into beta-sheets features in the formation of the scrapie prion proteins. Proc Natl Acad Sci USA 1993;90:10962–10966.
5. Riek R, Hornemann S, Wider G, Billeter M, Glockshuber R, Wüthrich K. NMR structure of the mouse prion protein domain PrP(121–231). Nature 1996;382:180–182.
6. Donne DG, Viles JH, Groth D, Mehlhorn I, James TL, Cohen FE, Prusiner SB, Wright PE, Dyson HJ. Structure of the recombinant full-length hamster prion protein PrP(29-231): the N terminus is highly flexible. Proc Natl Acad Sci USA 1997;94:13452–13457.
7. Zahn R, Liu A, Luhrs T, Riek R, von Schroetter C, Lopez Garcia F, Billeter M, Calzolai L, Wider G, Wüthrich K. NMR solution structure of the human prion protein. Proc Natl Acad Sci USA 2000;97:145–150.
8. Lopez Garcia F, Zahn R, Riek R, Wüthrich K. NMR structure of the bovine prion protein. Proc Natl Acad Sci USA 2000;97:8334–8339.
9. Calzolai L, Zahn R. Influence of pH on NMR structure and stability of the human prion protein globular domain. J Biol Chem. 2003;278:35592–35596.
10. Wille H, Michelitsch MD, Guénebaut V, Supattapone S, Serban A, Cohen FE, Agard DA, Prusiner SB. Structural studies of the scrapie prion protein by electron crystallography. Proc Natl Acad Sci USA 2002;99:3563–3568.
11. Thompson A, White AR, McLean C, Masters CL, Cappai R, Barrow CJ. Amyloidogenicity and neurotoxicity of peptides corresponding to the helical regions of PrP(C). J Neurosci Res 2000;62:293–301.
12. Caughey BW, Dong A, Bhat KS, Ernst D, Hayes SF, Caughey WS. Secondary structure analysis of the scrapie-associated protein PrP 27-30 in water by infrared spectroscopy. Biochemistry 1991;30:7672–7680.
13. Knaus KJ, Morillas M, Swietnicki W, Malone M, Surewicz WK, Yee VC. Crystal structure of the human prion protein reveals a mechanism for oligomerization. Nat Struct Biol 2001;8:770–774.
14. Welker E, Raymond LD, Scheraga HA, Caughey B. Intramolecular versus intermolecular disulfide bonds in prion proteins. J Biol Chem 2002;277:33477–33481.
15. Prusiner SB. Inherited prion diseases. Proc Natl Acad Sci USA 1994;91:4611–4614.
16. Chou PY, Fasman GD. Prediction of protein conformation. Biochemistry 1974;13:222–245.
17. Bosques CJ, Imperiali B. The interplay of glycosylation and disulfide formation influences fibrillization in a prion protein fragment. Proc Natl Acad Sci USA 2003;100:7593–7598.
18. Brown DR, Guantieri V, Grasso G, Impellizzeri G, Pappalardo G, Rizzarelli E. Copper(II) complexes of peptide fragments of the prion protein. Conformation changes induced by copper(II) and the binding motif in C-terminal protein region. J Inorg Biochem 2004;98:133–143.
19. Haire LF, Whyte SM, Vasisht N, Gill AC, Verma C, Dodson EJ, Dodson GG, Bayley P M. The crystal structure of the globular domain of sheep prion protein. J Mol Biol 2004;336:1175–1183.
20. Jones DT. Protein secondary structure prediction based on position-specific scoring matrices. J Mol Biol 1999;292:195–202.
21. McGuffin LJ, Bryson K, Jones DT. The PSIPRED protein structure prediction server. Bioinformatics 2000;16:404–405.
22. Muñoz V, Serrano L. Elucidating the folding problem of helical peptides using empirical parameters. II. Helix macrodipole effects and rational modification of the helical content of natural peptides. J Mol Biol 1994;245:275–296.
23. Muñoz V, Serrano L. Elucidating the folding problem of helical peptides using empirical parameters. II. Temperature and pH dependence. J Mol Biol 1994;245:297–308.
24. Muñoz V, Serrano L. Development of the multiple sequence approximation within the AGADIR model of α-helix formation: comparison with Zimm-Bragg and Lifson-Roig formalisms. Biopolymers 1997;41:495–509.
25. Lacroix E, Viguera AR, Serrano L. Elucidating the folding problem of α-helices: local motifs, long-range electrostatics, ionic-strength dependence and prediction of NMR parameters. J Mol Biol 1998;284:173–191.
26. Esposito C, Colicchio P, Facchiano A, Ragone R. Effect of a weak electrolyte on the critical micellar concentration of sodium dodecyl sulfate. J Colloid Interface Sci 1998;200:310–312.
27. Le Maire M, Champeil P, Møller JV. Interaction of membrane proteins and lipids with solubilizing detergents. Biochim Biophys Acta 2000;1508:86–111.
28. Kuroda Y, Maeda Y, Sawa S, Shibata K, Miyamoto K, Nakagawa T. Effects of detergents on the secondary structures of prion protein peptides as studied by CD spectroscopy. J Pept Sci 2003;9:212–220.
29. Fasman GD. Handbook of biochemistry and molecular biology, 3rd ed. CRC Press: Boca Raton; 1976. p 183–203.
30. Santoro MM, Bolen DW. Unfolding free energy changes determined by the linear extrapolation method. 1. Unfolding of phenylmethanesulfonyl alpha-chymotrypsin using different denaturants. Biochemistry 1988;27:8063–8068.
31. Eftink MR. The use of fluorescence methods to monitor unfolding transitions in proteins. Biophys J 1994;66:482–501.
32. Bordbar AK, Saboury AA, Housaindokht MR, Moosavi-Movahedi AA. Statistical effects of the binding of ionic surfactant to protein. J Colloid Interface Sci 1997;192:415–419.
33. Ambrosone L, Ragone R. The interaction of micelles with added species and its similarity to the denaturant binding model of proteins. J Colloid Interface Sci 1998;205:454–458.
34. Yang JT, Wu CSC, Martinez HM. Calculation of protein conformation from circular dichroism. Meth Enzymol 1986;130:208–269.
35. Zhong L, Johnson WC Jr. Environment affects amino acid preference for secondary structure. Proc Natl Acad Sci USA 1992;89:4462–4465.
36. Nelson JW, Kallenbach NR. Stabilization of the ribonuclease S-peptide α-helix by trifluoroethanol. Proteins 1986;1:211–217.
37. Nelson JW, Kallenbach NR. Persistence of the alpha-helix stop signal in the S-peptide in trifluoroethanol solutions. Biochemistry 1989;28:5256–5261.
38. Merutka G, Stellwagen E. Analysis of peptides for helical prediction. Biochemistry 1989;28:352–357.
39. Jasanoff A, Fersht AR. Quantitative determination of helical propensities from trifluoroethanol titration curves. Biochemistry 1994;33:2129–2135.
40. Schönbrunner N, Wey J, Engels J, Georg H, Kiefhaber T. Native-like β-structure in a trifluoroethanol-induced partially folded state of the all-β-sheet protein tendamistat. J Mol Biol 1996;260:432–445.
41. Buck M. Trifluoroethanol and colleagues: cosolvents come of age. Recent studies with peptides and proteins. Q Rev Biophys 1998;31:297–355.
42. Wu C S, Yang JT. Sequence-dependent conformations of short polypeptides in a hydrophobic environment. Mol Cell Biochem 1981;40:109–122.
43. Wu CS, Ikeda K, Yang JT. Ordered conformation of polypeptides and proteins in acidic dodecyl sulfate solution. Biochemistry 1981;20:566–570.
44. Tanford C. Protein denaturation. C. Theoretical models for the mechanism of denaturation. Adv Protein Chem 1970;24:1–95.
45. Wu JW, Wang ZX. New evidence for the denaturant binding model. Protein Sci 1999;8:2090–2097.
46. Schellman JA. Selective binding and solvent denaturation. Biopolymers 1987;26:549–559.

47. Koehl P, Levitt M. Structure-based conformational preferences of amino acids. Proc Natl Acad Sci USA 1999;96:12524–12529.
48. Hegde RS, Tremblay P, Groth D, DeArmond SJ, Prusiner SB, Lingappa VR. Transmissible and genetic prion diseases share a common pathway of neurodegeneration. Nature 1999;402:822–826.
49. Riek R, Wutrich K. Prion protein NMR structure and familial human spongiform encephalopathies. Proc Natl Acad Sci USA 1998;95:11667–11672.
50. Temussi PA, Masino L, Pastore A. From Alzheimer to Huntington: why is a structural understanding so difficult? EMBO J 2003;22: 355–361.
51. Ikeda K, Higo J. Free-energy landscape of a chameleon sequence in explicit water and its inherent α/β bifacial property. Protein Sci 2003;12:2542–2548.
52. Zhou X, Alber F, Folkers G, Gonnet GH, Chelvanayagam G. An analysis of the helix to strand transition between peptides with identical sequence. Proteins 2000;41:248–256.
53. Salmona M, Morbin M, Massignan T, Colombo L, Mazzoleni G, Capobianco R, Diomede L, Thaler F, Mollica L, Musco G, and others. Structural properties of Gerstmann-Sträussler-Scheinker disease amyloid protein. J Biol Chem 2003;28:48146–48153.
54. Ma J, Wollmann R, Lindquist S. Neurotoxicity and neurodegeneration when PrP accumulates in the cytosol. Science 2002;298:1781–1785.